ARTICLES
https://doi.org/10.1038/s41559-020-1136-3
nature ecology & evolution

Check for updates

A ^{14}C chronology for the Middle to Upper Palaeolithic transition at Bacho Kiro Cave, Bulgaria

Helen Fewlass[1]✉, Sahra Talamo[1,2], Lukas Wacker[3], Bernd Kromer[1,4], Thibaut Tuna[5], Yoann Fagault[5], Edouard Bard[5], Shannon P. McPherron[1], Vera Aldeias[1,6], Raquel Maria[1], Naomi L. Martisius[7], Lindsay Paskulin[8], Zeljko Rezek[1,9], Virginie Sinet-Mathiot[1], Svoboda Sirakova[10], Geoffrey M. Smith[1], Rosen Spasov[11], Frido Welker[1,12], Nikolay Sirakov[10], Tsenka Tsanova[1] and Jean-Jacques Hublin[1,13]

The stratigraphy at Bacho Kiro Cave, Bulgaria, spans the Middle to Upper Palaeolithic transition, including an Initial Upper Palaeolithic (IUP) assemblage argued to represent the earliest arrival of Upper Palaeolithic *Homo sapiens* in Europe. We applied the latest techniques in ^{14}C dating to an extensive dataset of newly excavated animal and human bones to produce a robust, high-precision radiocarbon chronology for the site. At the base of the stratigraphy, the Middle Palaeolithic (MP) occupation dates to >51,000 yr BP. A chronological gap of over 3,000 years separates the MP occupation from the occupation of the cave by *H. sapiens*, which extends to 34,000 cal BP. The extensive IUP assemblage, now associated with directly dated *H. sapiens* fossils at this site, securely dates to 45,820–43,650 cal BP (95.4% probability), probably beginning from 46,940 cal BP (95.4% probability). The results provide chronological context for the early occupation of Europe by Upper Palaeolithic *H. sapiens*.

Bacho Kiro Cave in Bulgaria (Fig. 1a) has an archaeological sequence spanning the late Middle Palaeolithic (MP) through the early Upper Palaeolithic (UP). First excavated in 1938[1] and again in 1971–1975[2], the cave is notable for its distinctive lithic assemblages from Layers 11 and 11a[2] consisting of elongated Levallois-like blades, retouched points, end-scrapers and splintered pieces, along with pendants made of animal teeth[2–4]. A radiocarbon date of >43,000 ^{14}C yr BP (GrN-7545) (Table 1) on charcoal from Layer 11 made it perhaps one of the earliest UP assemblages in Europe[2]. Originally named 'Bachokirian'[2], the assemblage is now recognized as part of the Initial Upper Palaeolithic (IUP)[3,5] and is argued to represent one of the earliest occurrences of UP *Homo sapiens* in Europe[4,6].

In 2015, the National Archaeological Institute with Museum (Sofia) and the Department of Human Evolution at the Max Planck Institute for Evolutionary Anthropology (MPI-EVA, Leipzig) reopened the cave with the primary goals of resampling the lithic assemblages and redating the IUP Layers 11 and 11a[7]. Two excavation sectors adjacent to the area of the 1970s excavations were established (Fig. 1b) and excavated to bedrock. The Main Sector (Fig. 1c) encompasses the sequence as previously described[2]. The Niche 1 is a small and low-ceilinged lateral chamber located to the east, preserving only the lower portion of the sequence, including the IUP and underlying MP (Fig. 1d). Layer designations were kept separate between these two areas, with the layers from Niche 1 having an 'N1-' prefix. The two areas are ~4 m apart (Fig. 1b and Extended Data Fig. 1). Previous excavations removed the deposits connecting the two sectors but field observations of sedimentary characteristics, morphology and archaeological content allow some layers to be correlated (Supplementary Text 1). Here, we use the new stratigraphic nomenclature (Fig. 1) wherein Layer 11[2] corresponds to Layer I in the Main Sector and Layer N1-I in the Niche 1 and Layer 11a[2] to Layers J and N1-J.

The recent excavations confirm the previously reported stratigraphy and archaeological sequence[2] (Extended Data Fig. 2). In the Main Sector (Fig. 1c), the stratigraphy begins with the upper part of Layer J, which overlies bedrock and continues through to Layer A0 at the current surface of the cave deposit. The Niche 1 stratigraphy (Fig. 1d) starts with Layer N1-K deposited directly on the bedrock, continuing through Layer N1-J and the distinctive Layer N1-I, into deposits ending with Layer N1-3a. On the basis of archaeological and geological observations, Layers N1-J, N1-I and N1-H/G in the Niche 1 clearly correspond, respectively, to Layers J, I and G in the Main Sector. The labelling of layers in the upper part of the Niche 1 stratigraphy with numbers (N1-3a–e) reflects the lack of correlation of these layers to lettered layers (A–J) in the Main Sector, although the erosive lower contact of Layers C and N1-3b can be used as a stratigraphic marker in these two areas.

Overall, the sequence is characterized by an exceptionally high artefact density in Layers I and N1-I (15 finds >2 cm l^{-1} of sediment) and low densities in other layers. During the new excavations, we recovered ~14,000 bones and ~2,000 lithics (>2 cm), with >70% of

[1]Department of Human Evolution, Max Planck Institute for Evolutionary Anthropology, Leipzig, Germany. [2]Department of Chemistry 'G. Ciamician', University of Bologna, Bologna, Italy. [3]Ion Beam Physics, ETH Zürich, Zürich, Switzerland. [4]Institute of Environmental Physics, University of Heidelberg, Heidelberg, Germany. [5]CEREGE, Aix-Marseille University, CNRS, IRD, INRA, Collège de France, Aix-en-Provence, France. [6]ICArEHB, University of Algarve, Campus de Gambelas, Faro, Portugal. [7]Department of Anthropology, University of California, Davis, CA, USA. [8]Department of Archaeology, University of Aberdeen, Aberdeen, UK. [9]University of Pennsylvania Museum of Archaeology and Anthropology, Philadelphia, PA, USA. [10]National Institute of Archaeology and Museum, Bulgarian Academy of Sciences, Sofia, Bulgaria. [11]Archaeology Department, New Bulgarian University, Sofia, Bulgaria. [12]Evolutionary Genomics Section, Globe Institute, University of Copenhagen, Copenhagen, Denmark. [13]Collège de France, Paris, France. ✉e-mail: helen_fewlass@eva.mpg.de

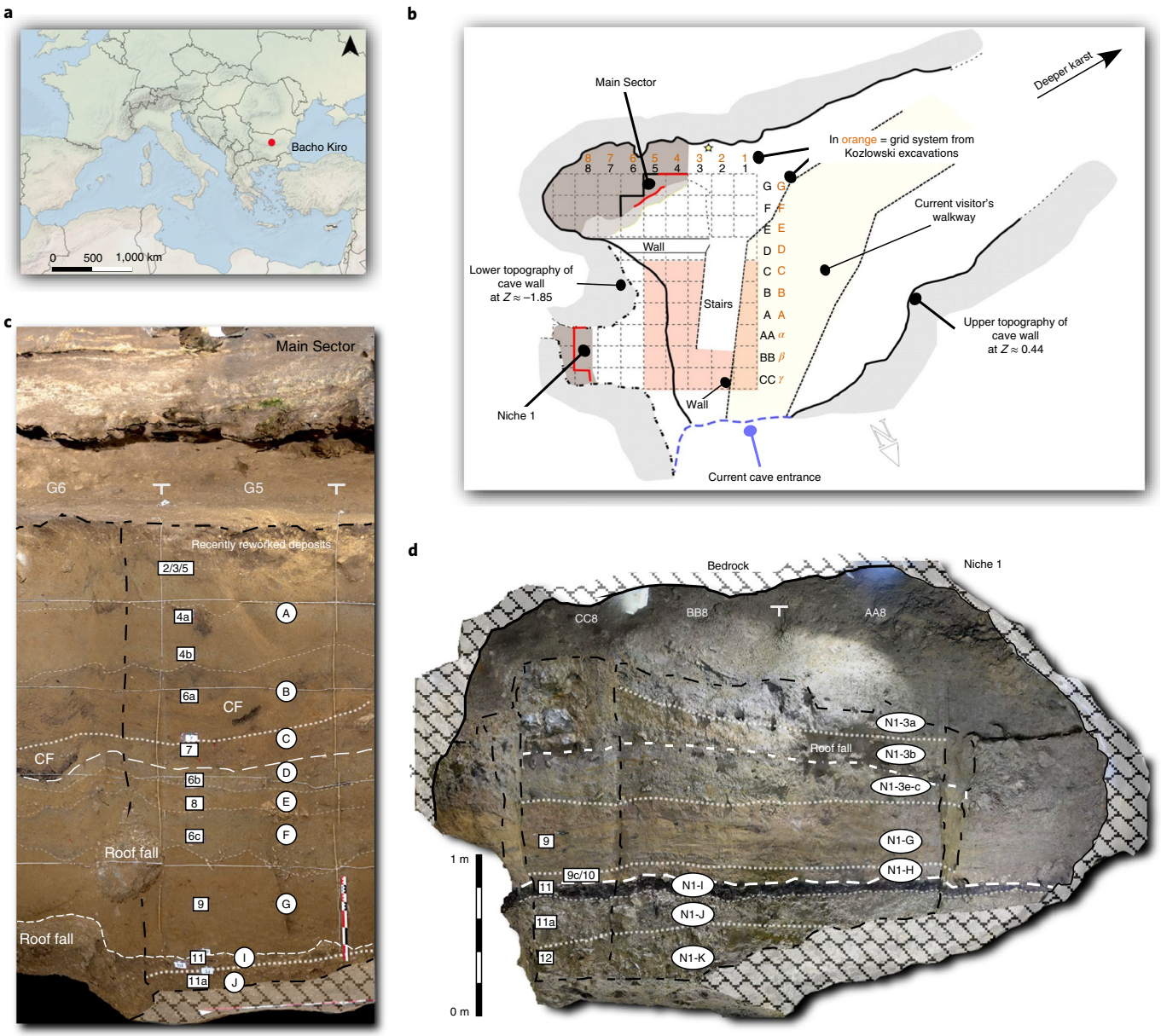

Fig. 1 | Bacho Kiro Cave. a, Location of the cave in Bulgaria, Balkan Peninsula, south-eastern Europe (base map from public domain map dataset naturalearthdata.com). **b**, Site plan showing the location of excavations carried out in 1971–1975 (centre, light orange) and the new excavations, in the Main Sector (top) and in the Niche 1 (left). *Z* is the elevation relative to the datum point. In **b**, the locations of the profiles shown in **c** and **d** are marked by red lines. **c**, Stratigraphic sequence in the Main Sector, along squares G5 and G6 in 2015. Note the presence of Layer J overlying the bedrock at the bottom of the sequence. **d**, Extract from a 3D model of Niche 1, showing the stratigraphic sequence. Layer attributions from this sector have an 'N1-' prefix. Note the distinctive dark colour of Layer N1-I. In **c** and **d**, numbers in white squares show the layer attributions from the 1970s excavations. Letters in white circles show the layer attributions from the recent excavations.

these coming from Layers I and N1-I. These quantities allow the lithic and bone industry to be correlated with previously excavated material and securely characterized as IUP[2,3] (Supplementary Table 1). In both the old and new lithic collections, the material from Layers J and N1-J is technologically consistent with the Layer I/N1-I assemblage but the find density is much lower (0.6 finds l^{-1} of sediment). The contact between N1-J and the underlying Layer N1-K is gradual, making the separation between the two sometimes difficult to recognize in the field, and there are some artefacts at the base of Layer N1-J that are consistent with the MP assemblage of the underlying Layer N1-K (Levallois flakes from coarse-grained syenite porphyry). In addition to changes in typology and technology from flakes to blades, this transition is marked by a shift in raw material use, from coarser syenite porphyry to fine-grained flint[2]. Layers G–D and N1-G–N1-3a contain no lithic artefacts and a very low density of animal bones. Layers C, B, A2 and A1 in the upper part of the stratigraphy contain characteristic UP artefacts, including retouched blades, backed bladelets, carinated end-scrapers, burins and bone tools. However, their lithic assemblages are poor in diagnostic technological attributes of any particular UP industry (Supplementary Table 1).

In the 1980s and 1990s, radiocarbon dating was attempted on material from the 1970s excavation[2,8]. Although several of the samples produced dates of great antiquity, the sequence of dates was

Table 1 | Previously published radiocarbon dates on material excavated from Bacho Kiro Cave during 1971–1975

Layer	Sample type	AMS laboratory number	^{14}C age (yr BP)	1σ error (yr)	Ref.
7	Charcoal	OxA-3181	32,200	780	8
6a/7	Bone	Ly1102	29,150	950	2,45
6b	Charcoal	OxA-3182	33,300	820	8
6b	Bone (no. 972)	GrN-7569	32,700	300	2
11	Charcoal from hearth	GrN-7545	>43,000		2
11	Bone	OxA-3213	38,500	1,700	8
11	Charcoal	OxA-3183	37,650	1,450	8
11	Tooth	OxA-3212	34,800	1,150	8
11a	Bone	OxA-3184	33,750	850	8
13	Bone (nos. 933 and 936)	GrN-7570	>47,000		2

inconsistent with the stratigraphy (Table 1). In particular, a wide range (>43,000–34,800 ± 1,150 ^{14}C yr BP) was obtained from Layer 11 and a younger date (33,750 ± 850 ^{14}C yr BP) from the underlying Layer 11a. This suggested that either the site was affected by post-depositional mixing between layers, or storage of the material was problematic, and/or that modern carbon contamination had been insufficiently removed from some of the samples before ^{14}C dating, leading to an underestimation of their true ages[8]. Since then the establishment of more stringent methods of sample pretreatment, including acid–base–wet oxidation pretreatment for charcoal[9,10] and ultrafiltration of bone collagen[11–13], have greatly improved the reliability of radiocarbon dates on Palaeolithic samples[14].

During ZooMS (Zooarchaeology by Mass Spectrometry)[15] screening of a subset of undiagnostic bone fragments from Bacho Kiro Cave, several elements from Layer N1-I (n = 4), Layer B (n = 1) and from the 1970s collection (Layer B/C; n = 1) were identified as hominin[4]. In 2017, a morphologically diagnostic hominin molar was found in Layer J in the Main Sector. DNA analysis confirmed the attribution of these seven elements to *H. sapiens*. The five newly identified *H. sapiens* from Layers N1-I and J, described in detail in Hublin et al.[4], are securely associated with the IUP assemblage and represent an early dispersal of *H. sapiens* into Europe in the UP. Given the implications of this assemblage, we sought to establish the range of the IUP at Bacho Kiro Cave and resolve the previous age anomalies by conducting a large-scale dating programme. In this paper, we present an extensive dataset of high-precision accelerator mass spectrometer (AMS) radiocarbon dates, which includes direct dating of the newly discovered *H. sapiens* bones[4].

Results

We successfully extracted collagen from 139 of the 147 pretreated bones (Supplementary Table 2). The average collagen yield across all layers was 8.3% with several bones in the lowest layers yielding up to 15% (Extended Data Fig. 3), which is much greater than the minimum level of 1% generally required for radiocarbon dating[16] and exceptional for a site of this age range. Isotopic and elemental analysis showed that all collagen extracts are within the range of well-preserved collagen, suitable for ^{14}C dating[16]. Although the C:N values of all extracts (range 3.0–3.4) were within the range of well-preserved collagen, four extracts had C% and N% values slightly above the normal range (marked in red in Supplementary Table 2), potentially indicating the presence of exogenous material. Only one of these was selected for dating and the age was identical to other bones in close proximity with acceptable C% and N% values. The Fourier transformed infrared (FTIR) spectra of all extracts were characteristic of pure collagen, with no evidence of exogenous material.

It has previously been suggested that the level of deamidation measured in ZooMS analysis could be an efficient prescreening tool to identify bones with well-preserved collagen for ^{14}C dating[17]. The large dataset in this study allowed us to robustly compare deamidation rates of two collagen peptides (P1106 and P1705) with collagen yields following extraction for ^{14}C dating. No correlation was observed between deamidation rates of peptides P1106 and P1705 and collagen yields, indicating that deamidation rates would be an unsuitable method for prescreening for ^{14}C sampling, at least for Bacho Kiro Cave (Supplementary Text 4 and Supplementary Fig. 5).

In total, we AMS dated 95 bones, including six *H. sapiens*. Of the dates obtained from animal bones, 63% are from specimens that were anthropogenically modified (Fig. 2 and Supplementary Text 5). The AMS measurements of the collagen backgrounds which were used in the age correction of all samples were highly reproducible within and between each magazine (~500 mg bone extractions: 2016 mean $F^{14}C = 0.00168$, s.d. = 0.00018; 2018 mean $F^{14}C = 0.00220$, s.d. = 0.00025; <100 mg bone extractions: 2018 mean $F^{14}C = 0.00291$; s.d. = 0.00034; Supplementary Table 3). Due to the high reproducibility of the background measurements, extended measurement time and high rate of transmission we were able to reach exceptional levels of precision. The finite dates span 49,430–27,250 cal BP (95.4% probability; Supplementary Tables 2, 4 and 5). Nine of the bones dated beyond the radiocarbon range (>51,000 yr BP). All of these come from the bottom of the stratigraphic sequence in the Niche 1, from Layer N1-K, the Layer N1-J/K contact and the lower part of Layer N1-J.

Eleven of the faunal collagen samples were dated in a second AMS laboratory (MAMS). The radiocarbon dates from the two laboratories are in statistical agreement for eight of the 11 samples (from Layers C, E, F and N1-I). However, combining dates from the two laboratories failed for three samples (R-EVA 1735, R-EVA 1737 and R-EVA 1739) from layer N1-I, all dating to >40,000 yr BP. The reasons for this are not understood so the dates were excluded from further analysis.

Extended Data Fig. 4 shows a comparison of the dates from graphite targets (~2.5 mg collagen) and the gas ion source (<0.3 mg collagen) of the Mini Carbon Dating System (MICADAS) system obtained for hominin bones F6-597 and BK-1653, carried out to cross-check the ages obtained. The level of precision achieved was excellent for both methods, despite a tenfold reduction in sample size using the gas ion source, and the dates from the different methods measured in two laboratories are in statistical agreement (Supplementary Table 6), lending reliability to the results.

After Bayesian modelling of the dates in OxCal[18,19], the agreement index was 80.4 for model 1 (Main Sector), 78.8 for model 2 (Niche 1), both above the generally accepted 60% threshold[20] (Supplementary Table 5). The high agreement index for the two separate areas indicates that the dates included are in keeping with their stratigraphic positions. The dates from Layers N1-I/I and N1-J/J support the archaeological and geological interpretations that these layers are correlated between the Main Sector and Niche 1. However, the different spatial accumulation of Layer J between the two areas results in a low agreement index (A_{model} = 28.9) for the model combining the dates (Supplementary Fig. 6). We therefore consider the Bayesian models of the two areas separately (Fig. 3; OxCal code in accompanying file).

Discussion

Over the past two decades, the addition of an ultrafiltration step following collagen extraction has shown to be important for removing carbon contamination from Palaeolithic bones[14]. The new Bacho Kiro Cave results indicate that several of the 1980s and 1990s dates

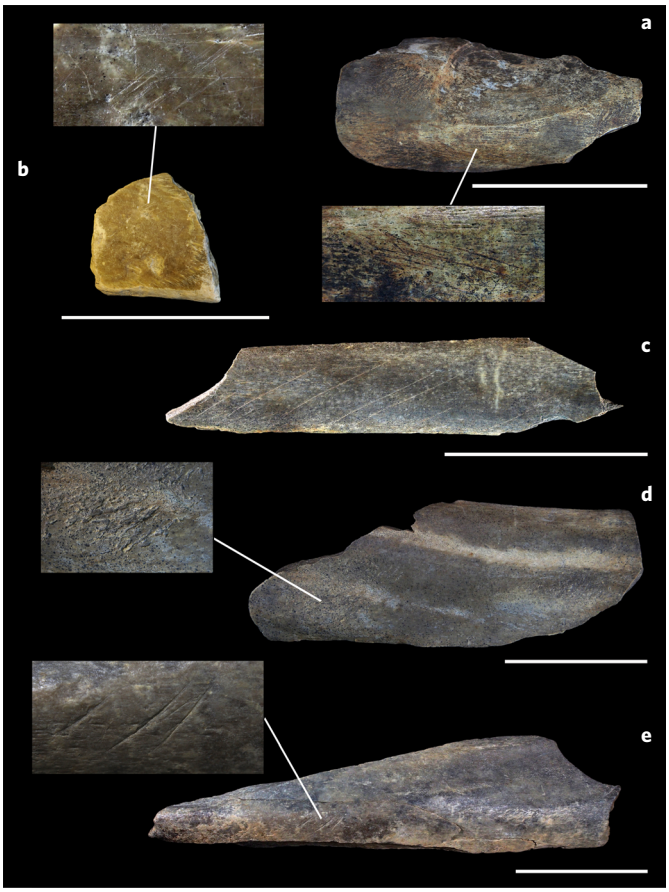

Fig. 2 | A selection of bone specimens from Bacho Kiro Cave with anthropogenic surface modifications that were radiocarbon dated in this study. a, *Equidae* bone (R-EVA 2298/CC7-2607) from the lower part of Layer N1-J with cut-marks (ETH-86787: 44,890 ± 450 ^{14}C yr BP). **b**, *Ursidae* bone (R-EVA 2290/BB8-207) from Layer N1-I with a large impact fracture scar, scrape marks and marks consistent with use as a retoucher (ETH-86783: 40,340 ± 280 ^{14}C yr BP). **c**, *Bos/Bison* rib (R-EVA 2352/F5-182) from the contact zone between Layers I and J in the Main Sector with parallel cut-marks (ETH-86813: 40,160 ± 270 ^{14}C yr BP). **d**, *Bos/Bison* long bone (R-EVA 2333/F5-107) excavated from Layer I used as a retoucher (ETH-86808: 41,350 ± 310 ^{14}C yr BP). **e**, *Bos/Bison* long bone (R-EVA 2311/CC7-2750) from layer N1-K with cut-marks (ETH-86793: >51,000 ^{14}C yr BP). Scale bars, 5 cm.

(Table 1) were affected by carbon contamination, making them appear younger than their actual ages. Our dates resolve the issues of the wide age range previously obtained for Layer I and the young age estimation obtained in Layer J (Table 1).

At the base of the sequence, resting on bedrock, Layer N1-K contains a small (n = 82) MP assemblage. All five dates from this layer are from *Cervid/Saiga* or *Bos/Bison* (including one with cut-marks) and are >51,000 yr BP. Overlying Layer N1-K, there are three age clusters represented in Layer N1-J, which accumulated relatively slowly (Supplementary Fig. 4). First, an anthropogenically modified *Ursidae* bone (ETH-86788) and a *Cervid/Saiga* bone (ETH-93195) from the very bottom of Layer N1-J are also >51,000 yr BP. Second, a minimum of 5,000 ^{14}C yr separates these two dates from the next occupation represented by a cut-marked horse bone (ETH-86787), also excavated from the lower part of Layer N1-J, indicating that hominins were present sometime between 49,430 and 46,940 cal BP (modelled age, 94.5% probability; Fig. 3b). A small number of lithics were recovered from the lower part of Layer N1-J. Some are consistent with the overlying IUP (n = 6) and some are consistent with the underlying MP (n = 8), which is in agreement with the findings of the 1970s excavations[2]. The gradual contact between N1-J and the underlying N1-K makes it difficult to clearly distinguish between the two layers during excavation of this area. From a radiocarbon perspective, it is impossible to know whether the lower part of Layer N1-J relates more to the overlying IUP or more to the underlying MP. However, the high resolution of the radiocarbon data suggests temporally distinct occupations in this lower part, which makes an in-situ transition between the MP and IUP less likely. The last occupation phase—in the upper part of Layer N1-J—spans from 46,940 to 45,130 cal BP (modelled range, 95.4% probability; Fig. 3b) and is associated with a low density of IUP artefacts which share the techno-typological characteristics of those in the overlying Layer N1-I. The dates from Layer J in the Main Sector (Fig. 3a) are at the younger end of the Layer N1-J range (95.4% modelled range: 45,690–44,390 cal BP), which supports the geoarchaeological interpretation that only the upper part of this layer is preserved in the Main Sector (where it overlies bedrock and abuts against it towards the south; Supplementary Text 1).

The appearance of the IUP in Layer N1-J coincides with a period of climatic warming indicated in various palaeoclimate records across the Northern Hemisphere, including the beginning of Greenland Interstadial 12 (GI12) at 46,950 ± 1,000 yr BP in the GICC05 NGRIP ice core[21] and beginning at ~47,600 yr BP in the Hulu Cave speleothem δ^{18}O records in China[22]. In closer proximity to Bacho Kiro Cave, mild climatic conditions are indicated in a speleothem δ^{13}C record from Ascunsa Cave (AC) in the South Carpathians[23] (~400 km northwest of Bacho Kiro Cave) and palaeoclimatic records from the Black Sea[24,25] and northern Greece[26]. However, correlations between calibrated ^{14}C dates and palaeoclimate archives linked to calendar ages are limited by the accuracy and precision in the calibration curve[27], especially approaching the limit of the method, and in the various palaeoclimate records themselves[28]. As such these correlations are tentative. Further work on local climatic conditions at Bacho Kiro Cave is ongoing and will be discussed further in future.

The evidence for the age range of Layer I/N1-I is extremely robust. Twenty-five dates on human remains and anthropogenically modified bones set the modelled age range for the IUP from these correlated layers from 45,820 to 43,650 cal BP (95.4% probability). The radiocarbon dates from the four dated *H. sapiens* bones span the full range of dates coming from anthropogenically modified bones. We chose to focus more on the dating of Layer N1-I in the Niche 1 where this layer is more extensively exposed and more clearly delineated in the stratigraphic sequence. Nevertheless, the four dates from Layer I in the Main Sector fall entirely within the range of Layer N1-I, supporting the archaeological and geological link made between these two areas. The dates from the contact zone I/J in the Main Sector fall within the range of Layer I and the upper part of Layer J. The age ranges from the upper part of Layer N1-J and from Layer N1-I, together with high artefact densities, imply relatively continuous human use of the cave during this interval. The radiocarbon evidence supports the archaeological and geological interpretation that Layer I represents an intensification of the IUP occupation that began during the formation of Layer J.

Site formation processes and the low number of artefacts in the layers above Layer I make it difficult to determine when the IUP ended at Bacho Kiro Cave. Layers N1-H, N1-G and G are thick water-laid deposits with a low density of artefacts at the base (Layers N1-H and G). These were probably redeposited from Layer N1-I/I by a stream originating from the cave's inner karst system. These layers essentially seal the underlying Layers N1-K, N1-J/J and N1-I/I[4]. Layers F and E are thick with very low densities of bones and no lithic artefacts. The tight age range from these layers overlap with the youngest age range of Layer I and suggest a rapid

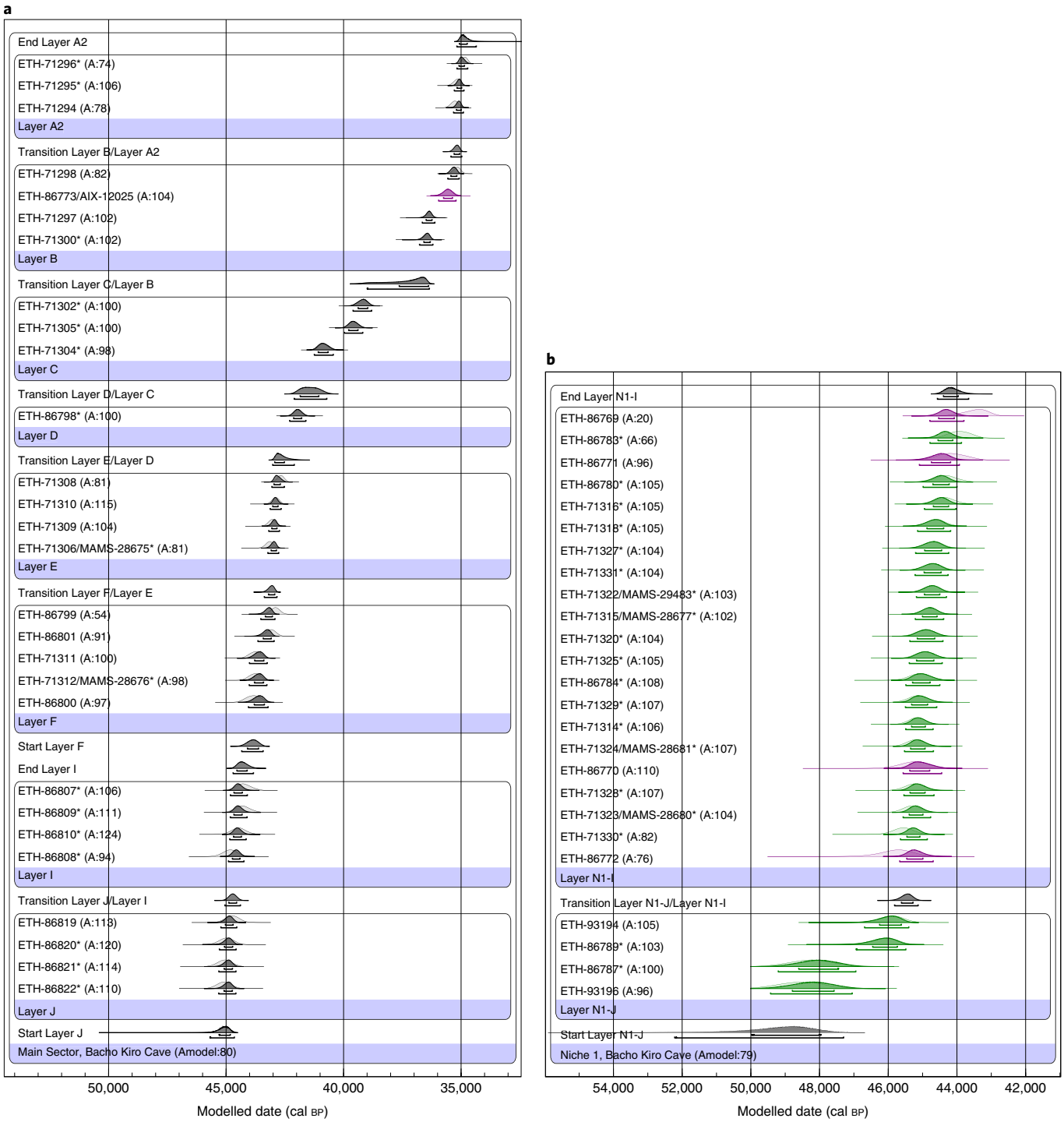

Fig. 3 | Bayesian chronological models for Bacho Kiro Cave. a,**b**, Material excavated during the 2015–2017 field seasons from the Main Sector (model 1) (**a**) and Niche 1 (model 2) (**b**). The AMS laboratory numbers are shown on the left side. The dates were calibrated against the IntCal13 dataset[19] and the modelling was performed in OxCal 4.3[18]. Where more than one measurement was made from the same collagen extract, dates were combined (R_Combine) in OxCal 4.3. The distributions of dates from the Niche 1 are shown in green and from the Main Sector in black. The dates from the *H. sapiens* bones from Layers N1-I and B are shown in purple. The radiocarbon likelihoods of calibrated dates (without modelling) are shown in the lighter shade and the posterior distributions (after modelling) are darkly shaded. Brackets show the 68.2% and 95.4% probability ranges of the calibrated dates. Dates marked with an asterisk (*) are from bones bearing signs of anthropogenic modification. Note that two further dates from the bottom of Layer N1-J date to >51,000 yr BP (beyond model range) as do two dates from the N1-J/K contact and five dates from the underlying Layer N1-K. Further information is included in Supplementary Tables 2, 4 and 5. OxCal code is included in Supplementary material.

rate of sedimentation for Layers G through E. Although no lithics were excavated from Layers F to D during the new excavations, the low density of artefacts recovered during the 1970s excavation indicate that the IUP characteristics continue from Layers J to D[4] (Supplementary Table 1). In the new collection, a relative increase in artefact density occurs in Layer C (42,110– 36,340 cal BP),

Layer B (39,000–34,970 cal BP) and Layer A2 (35,440–34,350 cal BP). The lithic artefacts within these layers are not characteristic of the IUP but rather of various phases of the subsequent UP (specifically bladelet production, platforms consistent with the appearance of soft hammer percussion in Layer C and backed bladelets similar to Gravettian types in Layer A1; Supplementary Table 1). In the Main Sector, the UP occupation extends to 34,350 cal BP (modelled range) in Layer A2. The date of 27,610–27,250 cal BP (95.4% probability) on a cut-marked *Bos/Bison* bone (ETH-86796) from Layer A1 is consistent with the associated Gravettian backed bladelets and makes this layer the youngest in the sequence. The Dansgaard-Oeschger climatic cycles in the Northern Hemisphere between the end of GI12 and the end of GI8 (~44,000–36,500 yr BP[21]) may have been a driver of the demographic turnover seen in archaeological and genetic studies during this interval in Europe[23,29], which is indicated at Bacho Kiro Cave by the change in technology seen between the IUP in Layers J and I and the UP forms in Layers C and above.

The Niche 1 has a shorter UP sequence than the Main Sector and the same differences in artefact densities. Nevertheless, we attempted to date the layers above Layer N1-I in part to help correlate its stratigraphy to that of the Main Sector. Unlike the rest of the deposits in this area, collagen preservation was very poor in these layers and only four of the 11 bones had sufficient collagen yields for dating. At least one of the resulting dates (ETH-86776 or ETH-86775) is inconsistent with its stratigraphic position (Supplementary Table 2) and it was not possible to make any connections between the upper layers of the Niche 1 and the Main Sector based on the radiocarbon evidence.

The date of the human bone F6-597 (35,960–35,210 cal BP, 95.4% modelled range) from Layer B agrees with the range of dates from the fauna in this layer. The hominin bone BK-1653 identified using ZooMS from the 1970s collection was labelled Layer '6a/7', which corresponds to the contact of Layers B and C in the new excavation. This bone was excluded from the modelling because of uncertainties over its exact stratigraphic context but its age (34,810–34,210 cal BP, 95.4% probability) fits with the dates on fauna from Layer A2. Both human bones from the UP levels of the site (BK-1653 and F6-597) were dated using both the gas ion source and graphite methods to cross-check the obtained ages (Extended Data Fig. 4 and Supplementary Table 6). The high level of agreement between the two methods measured in two different AMS laboratories serves as further evidence of the suitability of the gas ion source of the MICADAS for dating precious and/or small archaeological bone samples[30,31].

Conclusion

The chronology presented here for Bacho Kiro Cave constitutes an extensive set of high-quality collagen samples radiocarbon dated at exceptional precision. To the best of our knowledge, this study represents one of the largest ^{14}C datasets from a single Palaeolithic site processed by one team. This large effort was made to resolve the questions left open by the previous dates from this eponymous site. The integrity of the stratigraphic sequence is clearly indicated by the dates. The extensive dataset allows us to securely place the IUP from correlated Layers I and N1-I in the interval from 45,820–43,650 cal BP (95.4% probability). The start date for the IUP at Bacho Kiro Cave falls during the accumulation of Layer N1-J, probably sometime around 46,940 cal BP (95.4% probability). Direct radiocarbon dating of the four *H. sapiens* bones from Layer N1-I confirms their association with the IUP assemblage and represents the earliest direct evidence of our species in Europe in the UP.

Even as the precision of AMS measurements increases, one of the constraints of dating samples so close to the limit of the ^{14}C method is the imprecision of the calibration curve in this time range. The output of the Bayesian modelling presented here may change as the resolution of the calibration curve improves[22,32,33]. Ongoing work in this area is crucial for enhancing our understanding of the timing of major events in hominin adaptations and demographic processes during this time period.

Methods

Sample selection for radiocarbon dating. Bones were selected for radiocarbon dating from finds excavated during the 2015–2017 field seasons spanning the stratigraphy in both the Main Sector (Supplementary Figs. 1 and 2) and the Niche 1 (Supplementary Figs. 3 and 4). In total, 141 animal and six hominin bones were selected for collagen extraction (Supplementary Table 2). Where possible, animal bones that had signs of anthropogenic modification (cut-marks, impact fractures) on their surfaces were selected (53% of the sample set) (Fig. 2). A particular focus was given to sampling the IUP in Layer N1-I, where the layer was extensively exposed. Due to the exceptionally high density of bone in this layer (Supplementary Fig. 4), we were able to select a high number of bones (77%) with anthropogenic modifications. A small number of samples were also taken from Layer I in the Main Sector to confirm the stratigraphic link between the two areas through radiocarbon dating. During excavation of the contact zone between Layers I and J in the Main Sector, precise attribution of the finds to either Layer I or J was sometimes impossible to make, due to the sediment moistness and the presence of large limestone rubble. These finds are labelled as 'I/J' to indicate that they come from the contact zone between the sediments of these two layers.

Bone pretreatment. The bones were pretreated in the Department of Human Evolution at the MPI-EVA, following the collagen extraction plus ultrafiltration protocol described in Fewlass et al.[30] (see Supplementary Text 2 for further details). To preserve as much material as possible for ancient DNA and palaeoproteomic analysis, small aliquots of the hominin bones were sampled (80–110 mg) for direct ^{14}C dating. The quality of all the collagen extracts was assessed based on collagen yield, elemental (C%, N%, C:N) and stable isotopic values (δ^{13}C, δ^{15}N)[16]. All collagen extracts were analysed with FTIR spectroscopy before dating to look for evidence of incomplete demineralization, degraded collagen or the presence of any exogenous material in the extracts[34–36].

AMS measurement. Collagen extracts from six human bones and 89 animal bones and teeth were selected for radiocarbon dating based on stratigraphic position, signs of anthropogenic surface modification and the level of collagen preservation (Supplementary Table 2). The collagen extracts were graphitized using the AGE III[37] and dated using the MICADAS[38] in the Laboratory of Ion Beam Physics at ETH Zürich (laboratory code, ETH). The latest model of the MICADAS, equipped with helium stripping gas[39] and permanent magnets[40], has been in operation at ETH Zürich since the beginning of 2016 and produced high ion currents, a high rate of transmission, and a low and stable instrument background (~53,000 ^{14}C yr BP). Oxalic acid II standards and collagen backgrounds extracted alongside the samples were measured in the same magazine and used in the age calculation (AMS determinations of collagen and instrument backgrounds are included in Supplementary Table 3). Data reduction was performed using BATS software[41]. An additional 1‰ was added to the error calculation of the samples, as per standard practice.

Several collagen samples were split and dated in a second AMS laboratory to cross-check the measurements. Eleven fauna collagen samples plus collagen extraction backgrounds were weighed into cleaned tin cups and sent to the Klaus-Tschira-AMS facility in Mannheim (laboratory code, MAMS), where they were catalytically converted to graphite and dated with the MICADAS-AMS[42]. Here, data reduction was also carried out using BATS software[41], and errors were calculated from the blanks and standards measured in the same magazine. An additional 1‰ was included in the final error calculation, as per the standard practice at MAMS.

In addition to graphitization and AMS measurement at ETH Zürich, small aliquots of collagen (<100 µg C) from *H. sapiens* bones F6-597 and BK-1653 were measured using the gas ion source of the AixMICADAS[30,31,39] following the protocol described in Fewlass et al.[31].

Calibration and Bayesian modelling. Calibration and Bayesian chronological analysis was performed against the IntCal13 dataset[19] using OxCal 4.3[18]. Where multiple measurements were made from the same collagen extract, the R_Combine function in OxCal 4.3[18] was used to combine them. As part of this function, a chi-squared (χ^2) test is performed to see if the dates are in statistical agreement[43].

Some of the dates were excluded from the Bayesian chronological analysis: nine dating beyond 51,000 yr BP; four from the upper N1–3 layers; ten from the Layer I/J contact zone; three from Layer N1-I which failed the χ^2 test; one (ETH-71326) which was identified postexcavation as originating from next to the 1970s backfill; and the human bone (BK-1751) recovered from the 1970s collection as the context is not certain (Supplementary Table 2). Outlier analysis was performed for the rest of the dataset ($n = 67$) so that outliers could be manually eliminated[20]. Each layer was assigned a phase and we used a general outlier model with prior outlier probabilities set to 0.05[20]. As OxCal compresses posterior date distributions around the most precise date within a phase, the ordering of the data within each phase does not affect the model outcome so the dates were ordered chronologically rather than by stratigraphic depth. Dates from the Main Sector (model 1) and

Niche 1 (model 2) were first considered separately. As Layers I and J have been archaeologically and geologically correlated between the two areas, the dates were then combined in a third model (model 3). The likelihood of individual dates being outliers was considered based on their depositional histories, posterior outlier probabilities and individual agreement indices (<60% indicates the date could be incompatible with the model[20]) in the three models. On the basis of this information, 14 of the 67 dates (shown in red in Supplementary Table 4 and discussed in Supplementary Text 6) were identified as outliers. When the dates from the two areas were combined (model 3), a higher number of dates were identified as outliers but only those identified as outliers in the individual models were excluded from the final model. All models were then run again without outlier analysis with the spurious dates removed and were assessed based on the model agreement indices[20] (Supplementary Table 5).

ZooMS collagen fingerprinting. All specimens ($n=147$) in the radiocarbon study were also analysed using matrix-assisted laser desorption/ionization–time of flight mass spectrometry (MALDI-TOF-MS) collagen peptide mass fingerprinting[15,44] to provide accurate species identifications for each specimen (Supplementary Text 3).

Reporting Summary. Further information on research design is available in the Nature Research Reporting Summary linked to this article.

Data availability

All data are available in the manuscript and supplementary materials.

Code availability

OxCal script is included in the supplementary information.

Received: 30 July 2019; Accepted: 3 February 2020;
Published online: 11 May 2020

References

1. Garrod, D., Howe, B. & Gaul, J. Excavations in the cave of Bacho Kiro, north-east Bulgaria. *Bull. Am. Sch. Prehist. Res.* **15**, 46–76 (1939).
2. Kozłowski, J. K. *Excavation in the Bacho Kiro Cave (Bulgaria): Final Report* (Państwowe Wydawnictwo Naukowe, 1982).
3. Tsanova, T. *Les Débuts du Paléolithique Supérieur dans l'Est des Balkans. Réflexion à Partir de l'Étude Taphonomique et Techno-Économique des En-sembles Lithiques de Bacho Kiro (Couche 11), Temnata (Couches VI et 4) et Kozarnika (Niveau VII)* Vol. 1752 (BAR International Series, 2008).
4. Hublin, J. J. et al. Initial Upper Palaeolithic *Homo sapiens* remains from Bacho Kiro Cave (Bulgaria). *Nature* https://doi.org/10.1038/s41586-020-2259-z (2020).
5. Kuhn, S. L. & Zwyns, N. Rethinking the initial upper Paleolithic. *Quat. Int.* **347**, 29–38 (2014).
6. Hublin, J. J. The modern human colonization of western Eurasia: when and where? *Quat. Sci. Rev.* **118**, 194–210 (2015).
7. Sirakov, N. et al. *Reopened Bacho Kiro—new data on Middle/Upper Palaeolithic transition and Early-Middle stages of Upper Palaeolithic* (Bulgarian Academy of Sciences, 2017).
8. Hedges, R. E. M., Housley, R. A., Bronk Ramsey, C. & van Klinken, G. J. Radiocarbon dates from the Oxford AMS system: Archaeometry datelist 18. *Archaeometry* **36**, 337–374 (1994).
9. Bird, M. et al. Radiocarbon dating of 'old' charcoal using a wet oxidation, stepped-combustion procedure. *Radiocarbon* **41**, 127–140 (1999).
10. Wood, R. E. et al. Testing the ABOx-SC method: dating known-age charcoals associated with the Campanian Ignimbrite. *Quat. Geochronol.* **9**, 16–26 (2012).
11. Brown, T. A., Nelson, D. E., Vogel, J. S. & Southon, J. R. Improved collagen extraction by modified Longin method. *Radiocarbon* **30**, 171–177 (1988).
12. Bronk Ramsey, C., Higham, T., Bowles, A. & Hedges, R. Improvements to the pretreatment of bone at Oxford. *Radiocarbon* **46**, 155–164 (2004).
13. Talamo, S. & Richards, M. A comparison of bone pretreatment methods for AMS dating of samples >30,000 BP. *Radiocarbon* **53**, 443–449 (2011).
14. Higham, T. European Middle and Upper Palaeolithic radiocarbon dates are often older than they look: problems with previous dates and some remedies. *Antiquity* **85**, 235–249 (2011).
15. Buckley, M., Collins, M., Thomas-Oates, J. & Wilson, J. C. Species identification by analysis of bone collagen using matrix-assisted laser desorption/ionisation time-of-flight mass spectrometry. *Rapid Commun. Mass Spectrom.* **23**, 3843–3854 (2009).
16. van Klinken, G. J. Bone collagen quality indicators for palaeodietary and radiocarbon measurements. *J. Archaeol. Sci.* **26**, 687–695 (1999).
17. Wilson, J., van Doorn, N. L. & Collins, M. J. Assessing the extent of bone degradation using glutamine deamidation in collagen. *Anal. Chem.* **84**, 9041–9048 (2012).
18. Bronk Ramsey, C. Bayesian analysis of radiocarbon dates. *Radiocarbon* **51**, 337–360 (2009).
19. Reimer, P. J. et al. IntCal13 and Marine13 radiocarbon age calibration curves 0–50,000 years cal BP. *Radiocarbon* **55**, 1869–1887 (2013).
20. Bronk Ramsey, C. Dealing with outliers and offsets in radiocarbon dating. *Radiocarbon* **51**, 1023–1045 (2009).
21. Svensson, A. et al. A 60 000 year Greenland stratigraphic ice core chronology. *Clim. Past* **4**, 47–57 (2008).
22. Cheng, H. et al. Atmospheric $^{14}C/^{12}C$ changes during the last glacial period from Hulu Cave. *Science* **362**, 1293–1297 (2018).
23. Staubwasser, M. et al. Impact of climate change on the transition of Neanderthals to modern humans in Europe. *Proc. Natl Acad. Sci. USA* **115**, 9116–9121 (2018).
24. Nowaczyk, N. R., Arz, H. W., Frank, U., Kind, J. & Plessen, B. Dynamics of the Laschamp geomagnetic excursion from Black Sea sediments. *Earth Planet. Sci. Lett.* **351-352**, 54–69 (2012).
25. Wegwerth, A. et al. Black Sea temperature response to glacial millennial-scale climate variability. *Geophys. Res. Lett.* **42**, 8147–8154 (2015).
26. Müller, U. C. et al. The role of climate in the spread of modern humans into Europe. *Quat. Sci. Rev.* **30**, 273–279 (2011).
27. Giaccio, B., Hajdas, I., Isaia, R., Deino, A. & Nomade, S. High-precision ^{14}C and $^{40}Ar/^{39}Ar$ dating of the Campanian Ignimbrite (Y-5) reconciles the time-scales of climatic-cultural processes at 40 ka. *Sci. Rep.* **7**, 45940 (2017).
28. Buizert, C. et al. Abrupt ice-age shifts in southern westerly winds and Antarctic climate forced from the north. *Nature* **563**, 681–685 (2018).
29. Fu, Q. et al. The genetic history of Ice Age Europe. *Nature* **534**, 200–205 (2016).
30. Fewlass, H. et al. Size matters: radiocarbon dates of <200 µg ancient collagen samples with AixMICADAS and its gas ion source. *Radiocarbon* **60**, 425–439 (2017).
31. Fewlass, H. et al. Pretreatment and gaseous radiocarbon dating of 40–100 mg archaeological bone. *Sci. Rep.* **9**, 5342 (2019).
32. Talamo, S. et al. RESOLUTION: Radiocarbon, tree rings, and solar variability provide the accurate time scale for human evolution. In *Proc. of the European Society for the Study of Human Evolution* Vol. 6, 194 (ESHE, 2017); https://go.nature.com/2PnlI1h
33. Reimer, P. J. et al. A preview of the IntCal19 radiocarbon calibration curves. In *Book of Abstracts, 23rd International Radiocarbon Conference* 42 (2018); https://go.nature.com/3801Qb5
34. DeNiro, M. J. & Weiner, S. Chemical, enzymatic and spectroscopic characterization of "collagen" and other organic fractions from prehistoric bones. *Geochim. Cosmochim. Acta* **52**, 2197–2206 (1988).
35. Yizhaq, M. et al. Quality controlled radiocarbon dating of bones and charcoal from the early pre-pottery Neolithic B (PPNB) of Motza (Israel). *Radiocarbon* **47**, 193–206 (2005).
36. D'Elia, M. et al. Evaluation of possible contamination sources in the ^{14}C analysis of bone samples by FTIR spectroscopy. *Radiocarbon* **49**, 201–210 (2007).
37. Wacker, L., Němec, M. & Bourquin, J. A revolutionary graphitisation system: fully automated, compact and simple. *Nucl. Instrum. Methods Phys. Res. B* **268**, 931–934 (2010).
38. Wacker, L. et al. MICADAS: routine and high-precision radiocarbon dating. *Radiocarbon* **52**, 252–262 (2010).
39. Bard, E. et al. AixMICADAS, the accelerator mass spectrometer dedicated to ^{14}C recently installed in Aix-en-Provence, France. *Nucl. Instrum. Methods Phys. Res. B* **361**, 80–86 (2015).
40. Salehpour, M., Håkansson, K., Possnert, G., Wacker, L. & Synal, H.-A. Performance report for the low energy compact radiocarbon accelerator mass spectrometer at Uppsala University. *Nucl. Instrum. Methods Phys. Res. B* **371**, 360–364 (2016).
41. Wacker, L., Christl, M. & Synal, H.-A. Bats: a new tool for AMS data reduction. *Nucl. Instrum. Methods Phys. Res. B* **268**, 976–979 (2010).
42. Kromer, B., Lindauer, S., Synal, H.-A. & Wacker, L. MAMS—A new AMS facility at the Curt-Engelhorn-Centre for Achaeometry, Mannheim, Germany. *Nucl. Instrum. Methods Phys. Res. B* **294**, 11–13 (2013).
43. Ward, G. K. & Wilson, S. R. Procedures for comparing and combining radiocarbon age determinations: a critique. *Archaeometry* **20**, 19–31 (1978).
44. Welker, F. et al. Palaeoproteomic evidence identifies archaic hominins associated with the Châtelperronian at the Grotte du Renne. *Proc. Natl Acad. Sci. USA* **113**, 11162 (2016).
45. Evin, J., Marien, G. & Pachiaudi, C. Lyon natural radiocarbon measurements VII. *Radiocarbon* **20**, 19–57 (1978).

Acknowledgements

The re-excavation of Bacho Kiro Cave is a joint project between the National Institute of Archaeology and Museum, Bulgarian Academy of Sciences, Sofia and the Department of Human Evolution at the Max Planck Institute for Evolutionary Anthropology, Leipzig. This work was funded by the Max Planck Society. Graphitization and AMS dating in Switzerland were funded by ETH Zürich. The AixMICADAS and its operation are funded by the Collège de France and the EQUIPEX ASTER-CEREGE (Principle Investigator: E.B.). S.T. is funded by the European Research Council under the European

Union's Horizon 2020 Research and Innovation Programme (grant agreement No. 803147-951 RESOLUTION, awarded to S.T.). We acknowledge The National Museum of Natural History (Sofia), the Archaeology Department at New Bulgarian University (Sofia), the Regional Historical Museum in Gabrovo, the History Museum in Dryanovo and the guest house Platex in Dryanovo for their assistance in this project. We acknowledge the vital contribution of all the excavators who have worked at Bacho Kiro Cave since 2015.

Author contributions

The study was devised by J.-J.H., S.T., S.P.M., T. Tsanova, N.S. and H.F. Archaeological excavation was undertaken by T. Tsanova, N.S., Z.R., V.A. and S.P.M., who all contributed contextual information. The 2015–2017 excavation laboratory and collection was organized by V.S.-M. Lithic analysis was performed by T. Tsanova, N.S., S.S. and S.P.M. Zooarchaeological analysis was performed by G.M.S. and R.S. N.L.M. classified the bone tools in the sample set. Stratigraphic and micromorphological analysis was carried out by V.A. ZooMS was carried out by F.W., L.P. and V.S.-M. Sample pretreatment and EA-IRMS analyses were carried out by H.F. FTIR analyses were carried out by H.F. and R.M. Graphitization and AMS dating at ETH Zürich was carried out by L.W., B.K. and H.F. Dating with the AixMICADAS was carried out by E.B., Y.F. and T. Tuna. Bayesian modelling was carried out by H.F. and S.T. H.F. wrote the paper with input from all authors.

Competing interests

The authors declare no competing interests.

Additional information

Extended data is available for this paper at https://doi.org/10.1038/s41559-020-1136-3.

Supplementary information is available for this paper at https://doi.org/10.1038/s41559-020-1136-3.

Correspondence and requests for materials should be addressed to H.F.

Reprints and permissions information is available at www.nature.com/reprints.

Publisher's note Springer Nature remains neutral with regard to jurisdictional claims in published maps and institutional affiliations.

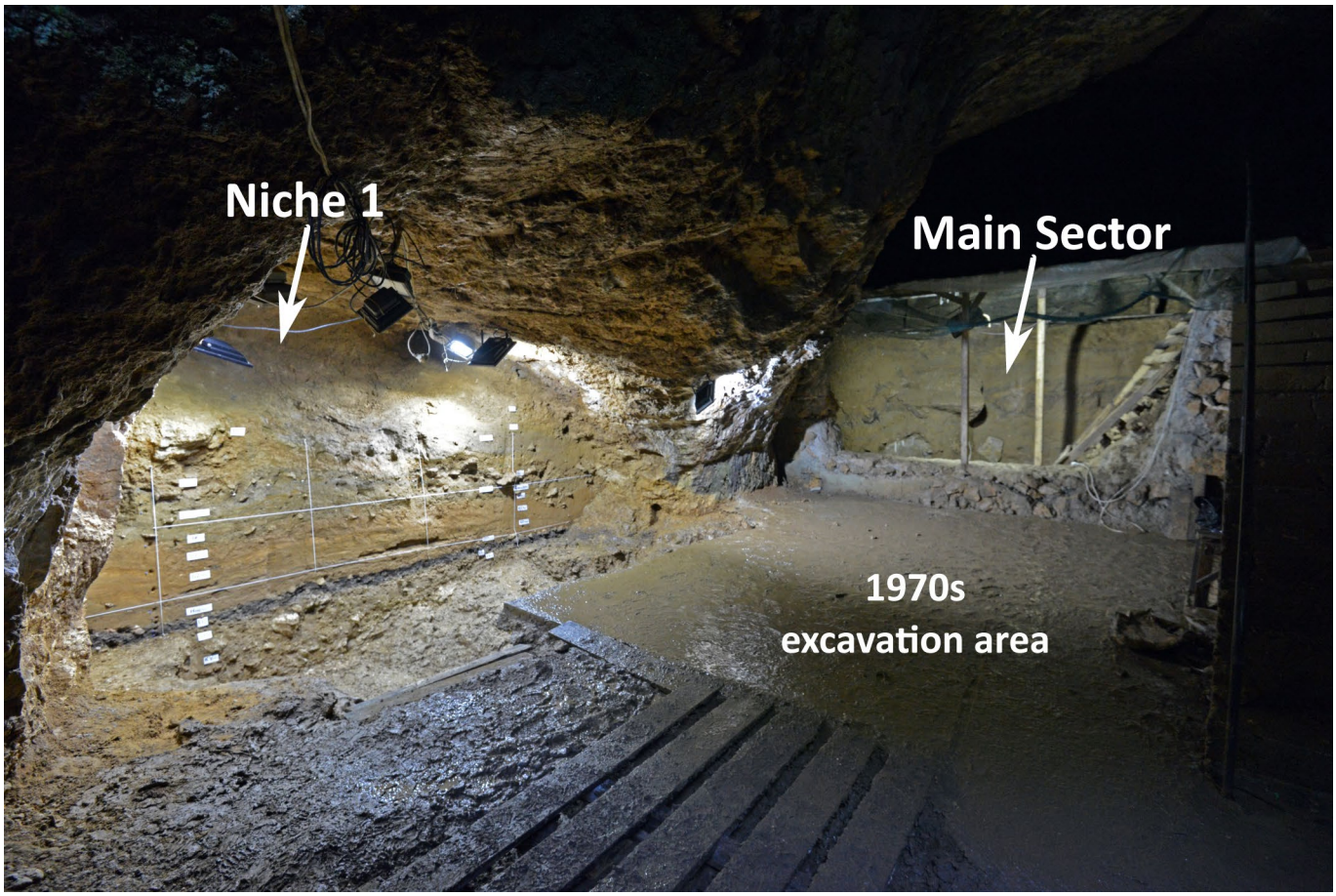

Extended Data Fig. 1 | Photograph of Bacho Kiro Cave excavations in 2019. View of the Niche 1 *(left)* and Main Sector *(right)*, looking toward the south in the cave. The concrete floor in the centre covers the 1970s excavation area.

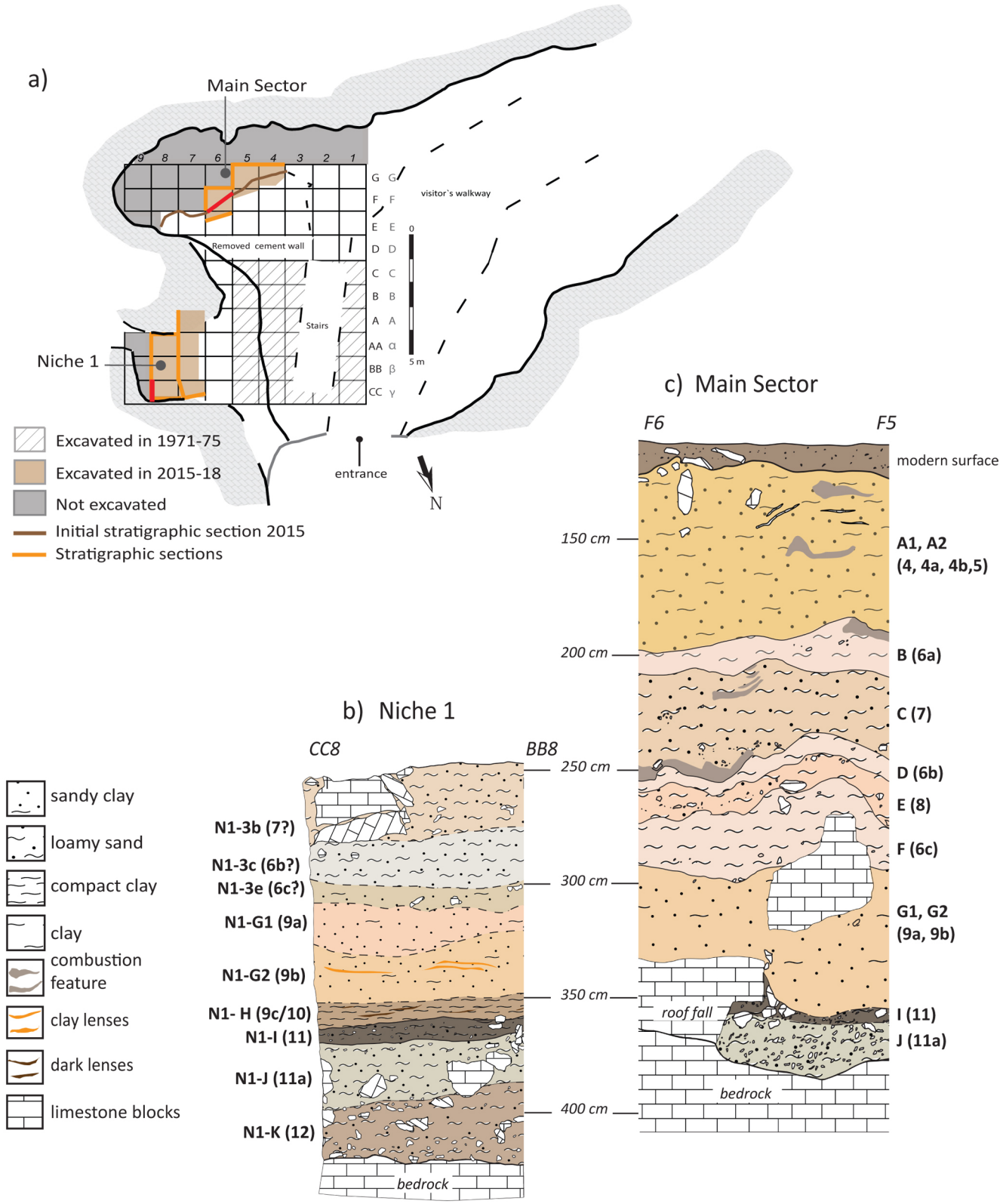

Extended Data Fig. 2 | Bacho Kiro Cave, excavation 2015-2018. a, Plan view of the entry hall and the excavated area, with the grid system of the recent excavations (black letters) and those of the 1971-75 excavations (grey letters). Red lines indicate the locations of the profile columns from Niche 1 (b) and Main Sector (c). **b**, Stratigraphic section-log in the Niche 1 in 2018. Layer attributions in the Niche 1 have an 'N1-' prefix. **c**, Initial stratigraphic section-log in the Main Sector in 2015. Numbers in parentheses show the layer attributions from the 1970s excavations. Legend for the stratigraphic units shown on the left.

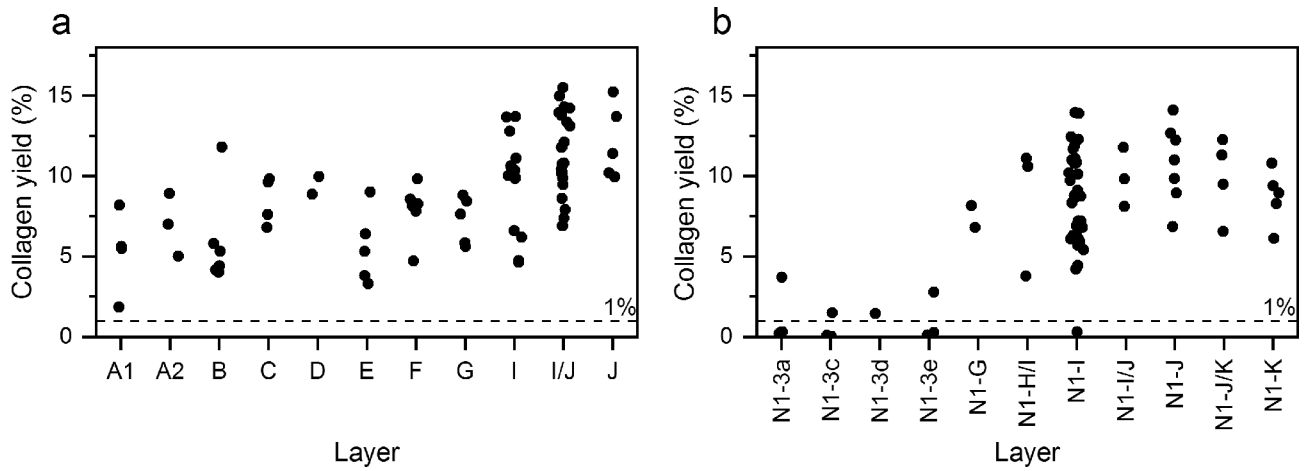

Extended Data Fig. 3 | Collagen yields (%) of pretreated bones. a, Main Sector and **b**, Niche 1, separated by layer and layer contact zones (I/J, N1-J/K, N1-I/J, N1-H/I). The dashed line shows the minimum level of collagen preservation generally considered suitable for ^{14}C dating.

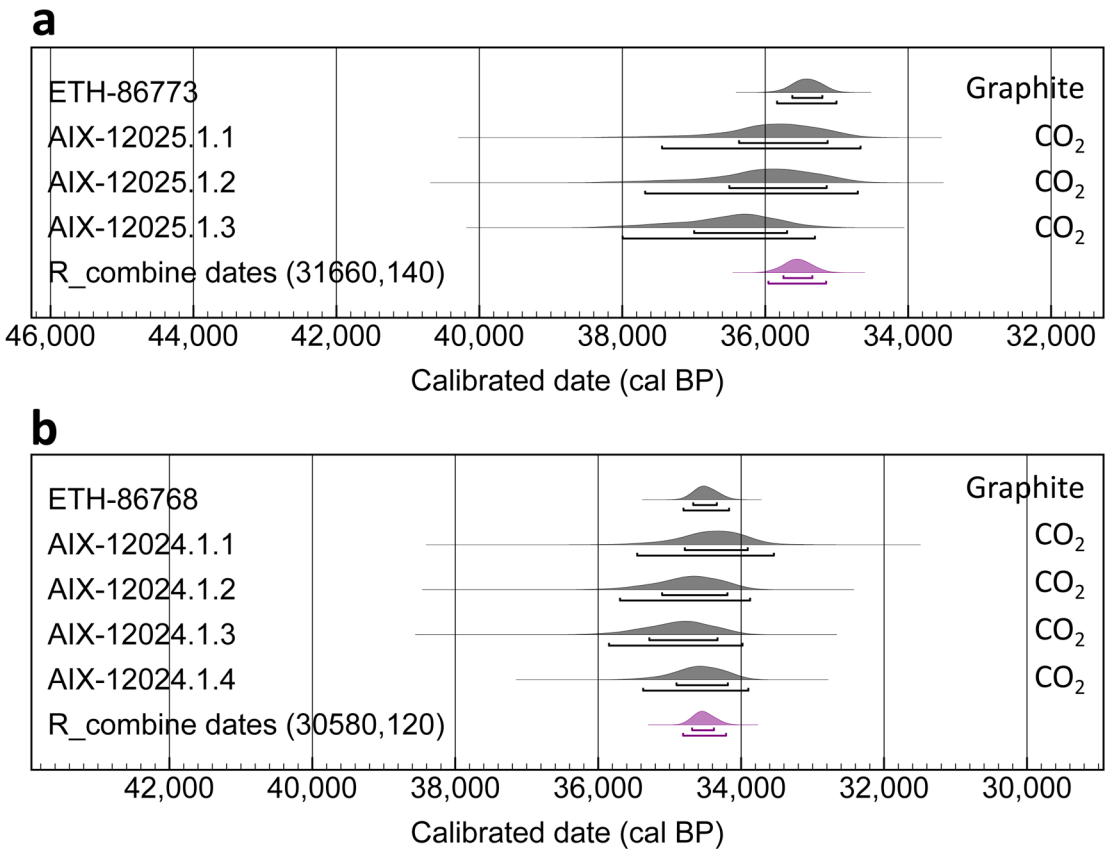

Extended Data Fig. 4 | Comparison of radiocarbon dates of *Homo sapiens* bones F6-597 and BK-1653. a, F6-597 comes from Layer B of the new excavations and **b**, BK-1653 comes from the 1970s collection (Layer 6a/7) that is stored in the National Museum of Natural History in Sofia. The purple range shows the weighted mean age and error of all the dates measured from graphite targets and directly from CO_2 gas (shown in Supplementary Table 6), calculated using the R_Combine function in OxCal 4.3[45].

nature research

Corresponding author(s): Helen Fewlass

Last updated by author(s): Jan 30, 2020

Reporting Summary

Nature Research wishes to improve the reproducibility of the work that we publish. This form provides structure for consistency and transparency in reporting. For further information on Nature Research policies, see Authors & Referees and the Editorial Policy Checklist.

Statistics

For all statistical analyses, confirm that the following items are present in the figure legend, table legend, main text, or Methods section.

n/a	Confirmed	
☐	☒	The exact sample size (*n*) for each experimental group/condition, given as a discrete number and unit of measurement
☐	☒	A statement on whether measurements were taken from distinct samples or whether the same sample was measured repeatedly
☐	☒	The statistical test(s) used AND whether they are one- or two-sided *Only common tests should be described solely by name; describe more complex techniques in the Methods section.*
☒	☐	A description of all covariates tested
☒	☐	A description of any assumptions or corrections, such as tests of normality and adjustment for multiple comparisons
☐	☒	A full description of the statistical parameters including central tendency (e.g. means) or other basic estimates (e.g. regression coefficient) AND variation (e.g. standard deviation) or associated estimates of uncertainty (e.g. confidence intervals)
☒	☐	For null hypothesis testing, the test statistic (e.g. *F*, *t*, *r*) with confidence intervals, effect sizes, degrees of freedom and *P* value noted *Give P values as exact values whenever suitable.*
☐	☒	For Bayesian analysis, information on the choice of priors and Markov chain Monte Carlo settings
☒	☐	For hierarchical and complex designs, identification of the appropriate level for tests and full reporting of outcomes
☒	☐	Estimates of effect sizes (e.g. Cohen's *d*, Pearson's *r*), indicating how they were calculated

Our web collection on statistics for biologists contains articles on many of the points above.

Software and code

Policy information about availability of computer code

Data collection	No software was used in data collection.
Data analysis	BATS 4.0, OxCal 4.3.

For manuscripts utilizing custom algorithms or software that are central to the research but not yet described in published literature, software must be made available to editors/reviewers. We strongly encourage code deposition in a community repository (e.g. GitHub). See the Nature Research guidelines for submitting code & software for further information.

Data

Policy information about availability of data

All manuscripts must include a data availability statement. This statement should provide the following information, where applicable:

- Accession codes, unique identifiers, or web links for publicly available datasets
- A list of figures that have associated raw data
- A description of any restrictions on data availability

All data is available in the manuscript and supplementary materials.

Field-specific reporting

Please select the one below that is the best fit for your research. If you are not sure, read the appropriate sections before making your selection.

☐ Life sciences ☐ Behavioural & social sciences ☒ Ecological, evolutionary & environmental sciences

For a reference copy of the document with all sections, see nature.com/documents/nr-reporting-summary-flat.pdf

Ecological, evolutionary & environmental sciences study design

All studies must disclose on these points even when the disclosure is negative.

Study description	New AMS radiocarbon dates from 95 newly excavated human and animal bones provide a full site chronology for Bacho Kiro Cave, spanning the Middle to Upper Palaeolithic transition.
Research sample	Collagen was extracted from archaeological bones from all stratigraphic levels of Bacho Kiro Cave.
Sampling strategy	147 bones+teeth from Bacho Kiro Cave were selected for collagen extraction from across all layers of the stratigraphy with a focus on the IUP layer in the Niche 1 area (Layer N1-I) where it was most extensively exposed. Bones were selected based on their size, level of preservation (physical appearance) and the presence of anthropological modifications (sampling was carried out in collaboration with zoo-archaeologists on-site). All bone+teeth samples were pretreated to extract and purify collagen. 95 collagen extracts were selected for AMS dating based on their level of preservation and quality (collagen weight yield, elemental data (C%, N%, C:N), FTIR analysis) and stratigraphic origin. Samples were chosen from across the archaeological layers with preference for samples with signs of anthropological modifications (which are taken to represent human presence in the cave). Radiocarbon dates were included in the Bayesian model based on outlier analysis.
Data collection	H. Fewlass collected the fauna samples in Dryanovo, Bulgaria, during the 2016 and 2017 archaeological excavation (May/June) and study (October) seasons and the human bones were sampled in the lab at the MPI-EVA in 2017.
Timing and spatial scale	Bones were excavated from the Niche 1 and Main Sector areas of Bacho Kiro Cave during the 2015/2016/2017 field seasons. Samples were collected during the 2016 and 2017 field/study seasons. Bone pretreatment and AMS dating of all samples was carried out over the course of 2016-2018. The year of excavation, year of pretreatment and sample provenience is given for all samples in Supplementary Table 2 and supplementary figures.
Data exclusions	Radiocarbon dates from some samples were excluded from the Bayesian modelling: 9 samples were outside modeling range (>51,000 BP); 4 from the upper N1-3 layers as they could not be linked to the stratigraphy in the Main Sector; 10 from the Layer I/J contact zone as they could not confidently be assigned to one phase; 3 from Layer N1-I which failed the $\chi 2$ test when AMS dates from two labs were combined; 1 which was identified post-excavation as originating from next to the 1970s backfill and therefore may not have been in its original context; and 1 which was taken from the 1970s collection (humna bone BK-1653). Outlier analysis was performed for the rest of the dataset (n=67) so that outliers (n=14) could be manually eliminated. Full details are given in the SI.
Reproducibility	Two AMS dating methods across three AMS labs were used to check reproducibility. 11 collagen extracts from different layers were dated with graphite targets on a MICADAS AMS at two labs (ETH-Zurich and MAMS). Results were in statistical agreement for 8 of the extracts. Dates from the two labs were outside 2 sigma for 3 of the oldest extracts (all >40,000 BP). These samples were excluded from further analysis. Collagen from two human bones was dated with graphite targets at ETH-Zurich and in replicate with the gas ion source of the Aix-MICADAS AMS at CEREGE. All measurements were in statistical agreement.
Randomization	N/A
Blinding	N/A

Did the study involve field work? ☒ Yes ☐ No

Field work, collection and transport

Field conditions	Excavations inside the cave in Bulgaria were carried out during May/June in 2015/2016/2017.
Location	All bones in the study were excavated from the Niche 1 and Main Sector areas in the entrance of Bacho Kiro Cave (42° 56′ 48″ N, 25° 25′ 49″ E), near Dryanovo, Bulgaria.
Access and import/export	Most of the sampling was performed in Dryanovo, Bulgaria. Temporary exports of some items were organized between Bulgaria and Germany. Permit delivered by National Museum of Natural History (Sofia) Nr. 4CH30/04.01.19.
Disturbance	The samples were obtained through archaeological excavation of two sections in the cave.

Reporting for specific materials, systems and methods

We require information from authors about some types of materials, experimental systems and methods used in many studies. Here, indicate whether each material, system or method listed is relevant to your study. If you are not sure if a list item applies to your research, read the appropriate section before selecting a response.

Materials & experimental systems

n/a	Involved in the study
☒	☐ Antibodies
☒	☐ Eukaryotic cell lines
☐	☒ Palaeontology
☒	☐ Animals and other organisms
☒	☐ Human research participants
☒	☐ Clinical data

Methods

n/a	Involved in the study
☒	☐ ChIP-seq
☒	☐ Flow cytometry
☒	☐ MRI-based neuroimaging

Palaeontology

Specimen provenance	All bones were excavated from Bacho Kiro Cave, Bulgaria, through a joint project of the National Archaeological Institute with Museum (NAIM-BAS, Sofia, Bulgaria) and the Department of Human Evolution at Max Planck Institute for Evolutionary Anthropology (MPI-EVA, Leipzig, Germany). Permission to excavate was authorized by the Ministry of Culture, Sofia (permit numbers: 124/11.05.2015; 225/28.04.2016; 47/02.05.2017; 99/17.04.2018).
Specimen deposition	The palaeontological collection will be deposited at the National Museum of Natural History in Sofia.
Dating methods	All samples were collected, pretreated and measured as part of this study. Collagen extraction and purification (including ultrafiltration) was carried out at the MPI-EVA, Leipzig using published protocols. The suitability of collagen extracts for measurement was assessed based on coll % yield, elemental data (C%, N%, C:N) and FTIR analysis. Quality criteria for all samples is included in the supplementary information. Samples were graphitised and measured with a MICADAS AMS at ETH-ZURICH and MAMS. Collagen samples were combusted and measured with the gas ion source of the Aix-MICADAS at CEREGE. Dates were calibrated and modeled using OxCal 4.3 using the IntCal13 dataset.

☒ Tick this box to confirm that the raw and calibrated dates are available in the paper or in Supplementary Information.

Terms and Conditions

Springer Nature journal content, brought to you courtesy of Springer Nature Customer Service Center GmbH (“Springer Nature”).
Springer Nature supports a reasonable amount of sharing of research papers by authors, subscribers and authorised users (“Users”), for small-scale personal, non-commercial use provided that all copyright, trade and service marks and other proprietary notices are maintained. By accessing, sharing, receiving or otherwise using the Springer Nature journal content you agree to these terms of use (“Terms”). For these purposes, Springer Nature considers academic use (by researchers and students) to be non-commercial.
These Terms are supplementary and will apply in addition to any applicable website terms and conditions, a relevant site licence or a personal subscription. These Terms will prevail over any conflict or ambiguity with regards to the relevant terms, a site licence or a personal subscription (to the extent of the conflict or ambiguity only). For Creative Commons-licensed articles, the terms of the Creative Commons license used will apply.
We collect and use personal data to provide access to the Springer Nature journal content. We may also use these personal data internally within ResearchGate and Springer Nature and as agreed share it, in an anonymised way, for purposes of tracking, analysis and reporting. We will not otherwise disclose your personal data outside the ResearchGate or the Springer Nature group of companies unless we have your permission as detailed in the Privacy Policy.
While Users may use the Springer Nature journal content for small scale, personal non-commercial use, it is important to note that Users may not:

1. use such content for the purpose of providing other users with access on a regular or large scale basis or as a means to circumvent access control;
2. use such content where to do so would be considered a criminal or statutory offence in any jurisdiction, or gives rise to civil liability, or is otherwise unlawful;
3. falsely or misleadingly imply or suggest endorsement, approval , sponsorship, or association unless explicitly agreed to by Springer Nature in writing;
4. use bots or other automated methods to access the content or redirect messages
5. override any security feature or exclusionary protocol; or
6. share the content in order to create substitute for Springer Nature products or services or a systematic database of Springer Nature journal content.

In line with the restriction against commercial use, Springer Nature does not permit the creation of a product or service that creates revenue, royalties, rent or income from our content or its inclusion as part of a paid for service or for other commercial gain. Springer Nature journal content cannot be used for inter-library loans and librarians may not upload Springer Nature journal content on a large scale into their, or any other, institutional repository.
These terms of use are reviewed regularly and may be amended at any time. Springer Nature is not obligated to publish any information or content on this website and may remove it or features or functionality at our sole discretion, at any time with or without notice. Springer Nature may revoke this licence to you at any time and remove access to any copies of the Springer Nature journal content which have been saved.
To the fullest extent permitted by law, Springer Nature makes no warranties, representations or guarantees to Users, either express or implied with respect to the Springer nature journal content and all parties disclaim and waive any implied warranties or warranties imposed by law, including merchantability or fitness for any particular purpose.
Please note that these rights do not automatically extend to content, data or other material published by Springer Nature that may be licensed from third parties.
If you would like to use or distribute our Springer Nature journal content to a wider audience or on a regular basis or in any other manner not expressly permitted by these Terms, please contact Springer Nature at

onlineservice@springernature.com